Water Infiltration and Storage affected by Subsoiling and Subsequent Tillage

Joseph L. Pikul, Jr.,* and J. Kristian Aase

ABSTRACT

Benefits of subsoiling are difficult to predict. Objectives were to (i) determine effect of subsoiling on water infiltration and storage and (ii) evaluate longevity of tillage-induced soil structure. Experiments were conducted during two years and on two soils that were not subsoiled (NoSS), subsoiled (SS), and subsoiled plus secondary tillage (SSplus). Soils were Dooley fine sandy loam and Williams loam (fine-loamy, mixed, superactive, frigid Typic Argiustolls) near Culbertson, MT. Subsoiling, to a depth of 0.3 m, in Exp. 1 was with a paratill and with parabolic shanks in Exp. 2. Secondary tillage was with a disk in Exp. 1 and with sweeps in Exp. 2. Infiltration was measured using a sprinkler infiltrometer. Final infiltration rate, after two simulated storms, was 14 mm h^{-1} on NoSS, 29 mm h^{-1} on SS, and 7 mm h^{-1} on SSplus. Penetration resistance (PR) measurements suggest that soil subsidence following simulated rainstorms was less on treatments with no secondary tillage. Average water drainage from the 1.83-m profile was 1.4 mm h^{-1} during the first 3 d after water application. Average drainage was 0.23 mm h^{-1} during Days 3 to 7 and 0.09 mm h^{-1} during Days 7 to 15. Regardless of improved water infiltration under SS, all soil profiles (1.83 m deep) drained to ≈444 mm of water in 15 d. Results reveal a difficult soil management problem. Subsoiling initially improves infiltration, but no additional water storage was discernable after 15 d. Further, excess water percolation has potential to leach nitrate-N from the profile.

Water limits crop production in the semiarid northern Great Plains of the USA. To successfully grow a crop every year it is essential to limit evaporative loss of water and maximize soil water storage. Water conservation measures are important for successful annual cropping on the semiarid northern Great Plains and, with careful management of soil and crops; continuous annual small grain production can be successful (Aase and Pikul, 1995; Aase and Schaefer, 1996). Summer fallow is commonly practiced to store water in the soil for use by a later crop (Haas et al., 1974). However, a high evaporation rate makes summer fallowing inefficient in storing water (Tanaka, 1985; Tanaka and Aase, 1987). Additionally, the fallow–wheat (*Triticum aestivum* L.) crop sequence has been implicated as the cause of serious declines in soil C (Rasmussen and Parton, 1994). Thus, careful management of soil and crops are key to efficient use of precipitation and maintenance of soil productivity.

Shallow soil pans can impede water and gas movement. Occurrence of pans may be a consequence of soil type or management or both. Many soils of the Southeastern Coastal Plain of the USA are weakly structured and prone to soil compaction (Busscher et al., 1986; Sojka et al., 1990). These loamy sands are easily compacted when exposed to traffic or other consolidation forces. Clay loams of the Southern Great Plains (Unger, 1993a) have dense Bt1 and Bt2 horizons that limit water infiltration and plant root penetration. Silt loams of the Pacific Northwest frequently have shallow layers of high strength that have been implicated as the cause of reduced water infiltration (Pikul et al., 1990) and poor plant performance (Sojka et al., 1993). Repeated shallow tillage of sandy loam soils in eastern Montana has elevated bulk density (ρ_b) and PR at a depth of 10 cm (Pikul and Aase, 1995). These pans are commonly referred to as tillage pans and are a consequence of pressure applied by normal tillage operations. The cases cited are but a small sample of typical pans that are mentioned in the literature. In each case, the cause of the pan and the climate were different, but tillage was sought as the means to loosen the pan and improve water relations and crop performance.

Objectives were to (i) determine effect of subsoiling on water infiltration and storage and (ii) evaluate longevity of soil structure created by tillage following three wetting and draining cycles.

MATERIALS AND METHODS

Experimental Site

Water infiltration experiments were conducted on a 32-ha research farm located 11 km north of Culbertson, MT, USA. Experiment 1 was within a Dooley fine sandy loam (fine-loamy, mixed, superactive, frigid Typic Argiustolls) mapping unit. Experiment 2 was within a Williams loam (fine-loamy, mixed, superactive, frigid Typic Argiustolls) mapping unit. Dooley and Williams soils are geographically associated. The Williams series consists of very deep, well drained, moderately slow or slowly permeable soils formed in calcareous glacial till. Williams soils are found on glacial till plains and moraines and have clay loam B2t horizons. The Dooley series consists of very deep, well-drained soils that formed in alluvium or eolian material 0.5 to 1 m deep over glacial till or lacustrine deposits. Dooley soils are on uplands and lacustrine areas and have sandy clay loam Bt horizons. In either case, below 0.3 m, considerable textural heterogeneity is typical (Aase and Pikul, 2000). For example, within a 1.2-ha parcel, mapped as Dooley fine sandy loam, Pikul and Aase (1998) reported soil textures of sandy loam, sandy clay, and sandy clay loam at the 0.3- to 0.6-m depth.

Annual precipitation at the research site was 357 mm, with ≈283 mm (80%) occurring during April through September. Plots were laid out on portions of the farm that had been managed in a fallow–wheat cropping sequence since about

J.L. Pikul, Jr., USDA-ARS, Northern Grain Insects Research Laboratory, 2923 Medary Ave., Brookings, SD 57006; J.K. Aase, USDA-ARS, Northwest Irrigation and Soils Research Laboratory, 3793 N. 3600 E., Kimberly, ID 83341, USA. Recieved 1 Apr. 2002. *Corresponding author (jpikul@ngirl.ars.usda.gov).

Published in Soil Sci. Soc. Am. J. 67:859–866 (2003).

Abbreviations: θ_v, soil water measurements; ρ_b, soil bulk density; NoSS, not subsoiled; SS, subsoiled; SSplus, subsoiled plus secondary tillage; PR, soil penetration resistance; SSI, soil subsidence index; SSR, soil strength response.

1975. Customarily, primary tillage was in the spring with a tandem disk or with medium-crown sweeps, 0.45 m wide, operated ≈0.1 m deep. Tillage for summer fallow was with sweeps at ≈0.1 m deep and rod weeder.

Subsoiling

Experiment 1 was a randomized complete block, with three replications. Tillage treatments were: (i) SS with paratill, (ii) subsoil with paratill and secondary tillage with disk (SSplus), and (iii) NoSS. Infiltration plots were ≈15 m long and 12 m wide. The paratill subsoiler had four shanks (two left facing and two right facing) with point spacing at 0.66 m. Our implement was similar to that illustrated by Unger (1993b, Fig. 1 and 3). Speed was ≈1.3 m s^{-1} and depth of subsoiling was ≈0.3 m. Disk tillage was ≈0.1 m deep. Tillage was conducted in early September and field measurements were terminated at the end of October.

Experiment 2 was a randomized complete block with four replications. These plots were established outside of the area used for studies in Year 1 for Exp. 1. Customary fallow tillage was deferred to avoid disturbance of standing wheat residue from the previous crop. Herbicides were used to kill plants on the infiltration plots. Tillage treatments were: (i) ripped with parabolic subsoiling shanks to a depth of 0.3 m (SS), (ii) ripped and tilled with subsurface sweeps (SSplus), and (iii) NoSS. Sweep tillage was ≈0.1 m deep. Tillage was conducted in mid-May and all field measurements were completed by the end of July.

Water Infiltration

A Palouse rainfall simulator (Bubenzer et al., 1985) was used to apply water at a rate of ≈40 mm h^{-1} to 1.16- by 1.16-m infiltration frames. Electrical conductivity of Missouri River water (Culbertson, MT, municipal water supply) used for the infiltration tests was 0.7 dS m^{-1}, concentration of cations was 0.157 g L^{-1}, and SAR was 13.6. This simulator was designed to mimic low intensity rainfall characteristics of the inland Pacific Northwest. Typical summer rainstorms in the northern Great Plains are high intensity and short duration. The Palouse simulator produces drop sizes that are ≈1.3 to 1.8 mm diameter. By comparison, natural rainfalls with intensities of ≈50 mm h^{-1} have drop sizes that are ≈1 to 5 mm in diameter (Wischmeier and Smith, 1958). Therefore, the test soil was not exposed to rainfall energy that exceeded that of naturally occurring storms.

Infiltration frames were constructed of heavy gauge steel. Frames were placed so that the path of only one subsoiling shank was within each infiltration frame. To install a frame to a depth of at least 0.3 m, we carefully dug a trench around the outside of the frame. As layers of soil were removed, the infiltration frame was forced downward to enclose an undisturbed soil monolith. Particular attention was given to soil outside the frame in the vicinity of the soil disturbance created by subsoiling shanks. This soil was removed, backfilled, and packed to eliminate lateral flow of water from inside the frame to outside the frame. Inside edges of the infiltration frames were sealed with bentonite clay to prevent any water leakage along the metal-soil interface. Frames were installed on each replication of each tillage treatment.

Surface conditions within infiltration frames on each treatment were protected from rainfall energy of naturally occurring storms during the course of both Exp. 1 and 2. Calibration pans were placed over the infiltration frames when rain was likely. Following infiltration tests, the frames were kept covered to minimize evaporative water loss.

Water application rate from the rainfall simulator was measured at the start and finish of each infiltration test by collecting the water from a 1.35-m^2 calibration pan placed over the infiltration frame. Application rate was calculated as the average of these measurements. Water infiltration was calculated as the difference between application rate and runoff rate. Ponded water (water that would have run off) was removed from within the infiltration frame by vacuum. Water was applied for 3 h on Day 1, 2, and 3. The soil drained for ≈20 h following each water application. Tests on NoSS for Exp. 1 in Year 1 were left unfinished because of the onset of winter weather. Thus, only duplicate measurements for Day 1 and 2 of infiltration tests are shown for Exp. 1.

Profile Water Content

Soil water content was measured using neutron attenuation in Exp. 2. Equipment was calibrated as described by Pikul and Aase (1998). Within each infiltration frame, a permanent access tube was installed, enabling volumetric soil water measurements to a depth of 2.0 m at 0.1-m increments. A ring of bentonite clay around and overlain with a small mound of soil prevented water from ponding and running down the soil-tube interface during infiltration tests. Soil water content was expressed as an average of four replications for each tillage treatment. Measurements were made before and after each of the three infiltration runs and at 1, 5, and 15 d following the last water application.

Penetration Resistance, Soil Water, and Bulk Density

Soil PR was measured with a Soiltest CL-700 pocket penetrometer for Exp. 1. This penetrometer has a blunt tip of 6.35-mm diameter. Before use, the penetrometer was calibrated against a load cell (Bradford, 1980) and measurements are presented as soil PR. Penetration resistance profiles to a depth of 0.44 m were obtained by excavating a trench perpendicular to the direction of tillage. This trench was dug through the area of the infiltration test ≈7 d after the last water application. On the trench wall, facing the infiltration test area, a 25-mm grid was established having width (horizontal component) of 0.42 m and length (vertical component) of 0.44 m. Within the grid, we measured PR at 306 points.

Samples for ρ_b and gravimetric water (Gardner, 1986) were obtained by extracting a 25-mm core horizontally from a freshly prepared face of the trench wall. The sampler had a cutting tip of 19.6 mm and three cores were bulked per depth. Sample depths were centered at 0.013 m and at 30-mm increments from a depth of 0.05 m to a depth of 0.38 m. Cores were taken from the path of the subsoiler. Gravimetric water content was determined on each increment. Volumetric water content was calculated as the product of ρ_b and gravimetric water content.

Penetration resistance for Exp. 2 was measured with a 30° cone penetrometer that had a base area of 645 mm^2. Measurements were taken within each frame at spatial-intervals of 0.10 m along each 0.9-m transect (nine positions). A depth profile of PR was obtained at increments of 0.075 m to a depth of 0.38 m (six depths). In each frame there were two transects oriented perpendicular to the direction of tillage, and penetrometer resistance measurements for like depth and transect positions were averaged.

Soil ρ_b and gravimetric water were each measured on the same day as PR. Bulk density samples were taken with a tube sampler described by Allmaras et al. (1988). The sampler had a cutting tip of 19.6 mm. Four cores were taken vertically within each infiltration frame in positions not disturbed by ripping. Each 0.30-m core was cut into ten 0.03-m depth incre-

ments. Gravimetric water content was determined on each increment and volumetric water content was calculated.

Soil subsidence is defined as the downward movement of the soil surface caused by the collapse of underlying tillage-induced macroporosity. Tilled soil subsides due to factors acting on the soil surface or within the tilled layer (Onstad et al., 1984). A single-value index of soil subsidence was calculated using PR data arrays from each treatment (Pikul and Aase, 1999). Surface maps using transect position, depth, and PR were prepared for each plot sampled in Exp. 1 and 2. Briefly, a three-dimensional plot of PR data yielded a response surface showing spatial variation of soil strength. Smoothed surface maps were prepared using three-dimensional surface plotting (Surfer 8, Golden Software Inc., Golden, CO). Default geostatistical gridding method of kriging was used to smooth PR data arrays. Standard deviation of residuals [PR(raw data)-PR(smooth data)] provided a way to evaluate the fit of each map to the original data.

Soil strength response (SSR), in units of force, was calculated for each smoothed surface in a manner analogous to calculating volume. Strength response was defined as the product of (transect length, m) × (soil depth, m) × (cone index, Pa) and had the units of force (N). Surfer software provides numerical integration procedures for calculating volume. Relative error was estimated by comparing numerical results from three numerical integration methods.

Nondimensional soil subsidence indices (SSIs) were calculated as:

$$SSI = (CONTROL_{SSR} - TRT_{SSR})/CONTROL_{SSR}, \quad [1]$$

where $CONTROL_{SSR}$ was the SSR value between a lower surface defined by PR = 0 and the smoothed surface of the NoSS treatment, and TRT_{SSR} was the SSR value between a lower surface defined by PR = 0 and the smoothed surface of either the SS or SSplus treatment. Soil subsidence index approaches zero as differences between control and treatment become less. All calculations were based on PR measured after three simulated rain events.

In a previous study, SSI was used to estimate soil subsidence 2.5 yr after subsoiling (Pikul and Aase, 1999). Positive values from that study ranged from 0.049 to 0.314. A normal probability plot of SSI using the Ryan-Joiner goodness-of-fit test (Minitab Statistical Software, Minitab Inc. State College, Pa) suggests a normal distribution ($p = 0.1$) of SSI values.

Values of final infiltration rate, cumulative infiltration, change in soil water content, and subsidence index were tested for significance using ANOVA and LSD.

RESULTS AND DISCUSSION

Bulk Density and Volumetric Water

Soil ρ_b and volumetric water for SSplus, SS, and NoSS treatments in the top 0.4 m are shown in Fig. 1 (Exp. 1) and Fig. 2 (Exp. 2) after the third water application. Comparison of Fig. 1 (NoSS) and Fig. 2 (NoSS) shows that there was a zone of maximum ρ_b at ≈0.10 m on the test plots for both Exp. 1 and 2. This maximum value was 1.64 and 1.74 Mg m^{-3}, respectively, for Exp. 1 and 2.

In the upper 0.1 m of the Dooley fine sandy loam (Exp. 1), sand content averaged 720 g kg^{-1} and clay content averaged 120 g kg^{-1}. In the upper 0.1 m of the Williams loam (Exp. 2), sand content averaged 650 g kg^{-1} and clay content averaged 170 g kg^{-1} (Fig. 3). Soil organic C in the top 0.03 m was ≈10 g kg^{-1}. We think that the zone of maximum ρ_b at ≈0.1 m depth was a consequence of the historic use of shallow sweep tillage on this farm and not a consequence of soil textural differences.

There are inherent problems associated with measurement of soil ρ_b in tillage studies because unconsolidated soil having large clods is difficult to sample. Soil ρ_b is necessary for volumetric water determination, and volumetric water is necessary for interpretation of PR

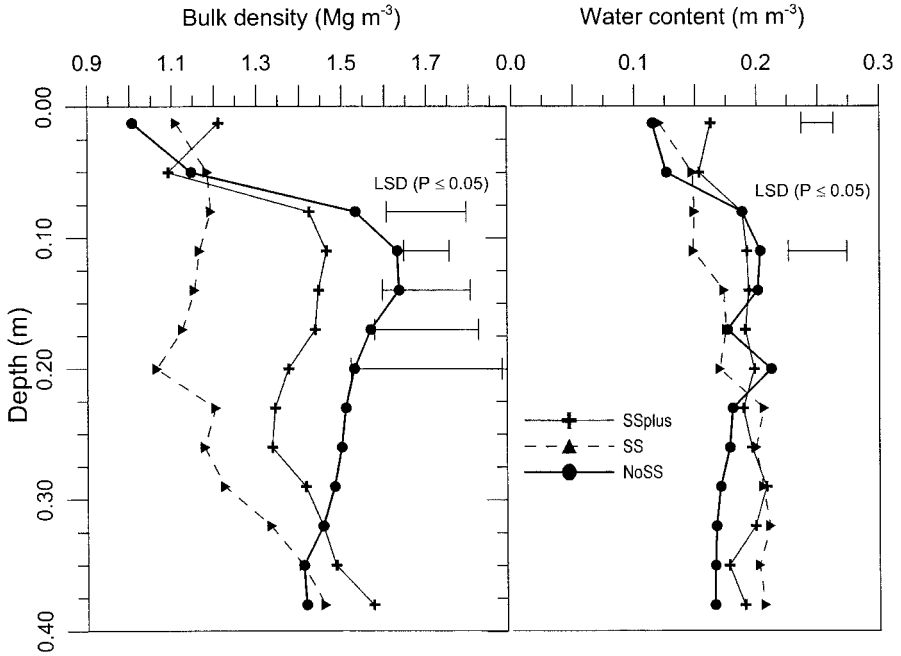

Fig. 1. Soil bulk density and volumetric water content ≈7 d after the last water application in Exp. 1 (Dooley fine sandy loam). Samples were taken centered on the path of the subsoiler. Tillage treatments were: (i) subsoiling with a paratill and secondary tillage with a disk (SSplus), (ii) subsoiling with a paratill (SS), and (iii) not subsoiled (NoSS). Least significant differences are shown where $P \leq 0.05$.

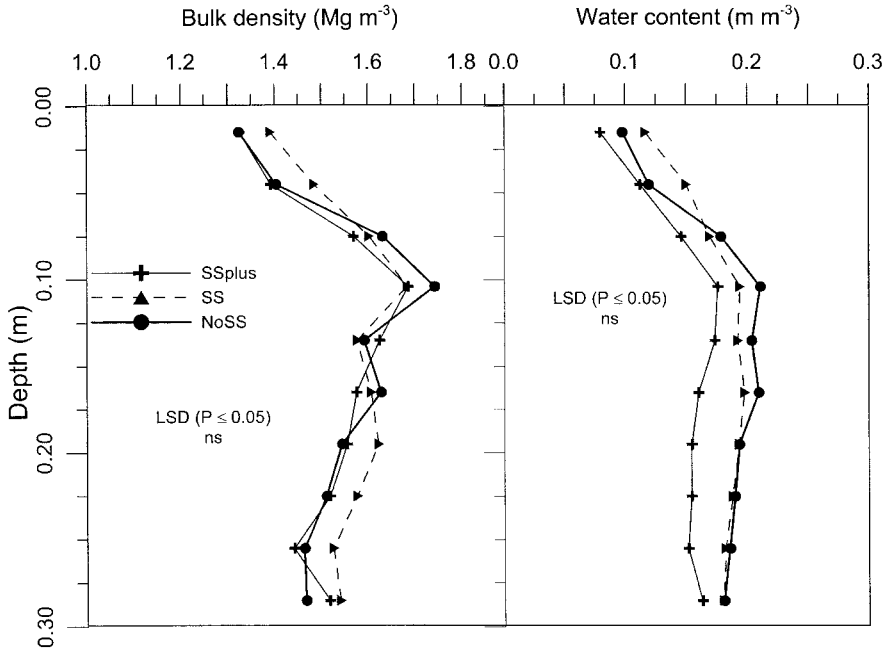

Fig. 2. Soil bulk density and volumetric water content ≈7 d after the last water application in Exp. 2 (Williams loam). Samples were taken off-center from the path of the subsoiler. Tillage treatments were: (i) subsoiling with parabolic subsoiling shanks and secondary tillage with sweeps (SSplus), (ii) subsoiling with parabolic subsoiling shanks (SS), and (iii) not subsoiled (NoSS). Least significant differences are shown where $P \leq 0.05$.

measurements. We used two methods to obtain soil samples from the tillage zone. In Exp. 1, samples were extracted horizontally after excavating a pit. In Exp. 2, profile samples were extracted by vertical sampling. The methodology used in Exp. 1 provided a way to accurately measure ρ_b within the path of subsoiling (Fig. 1).

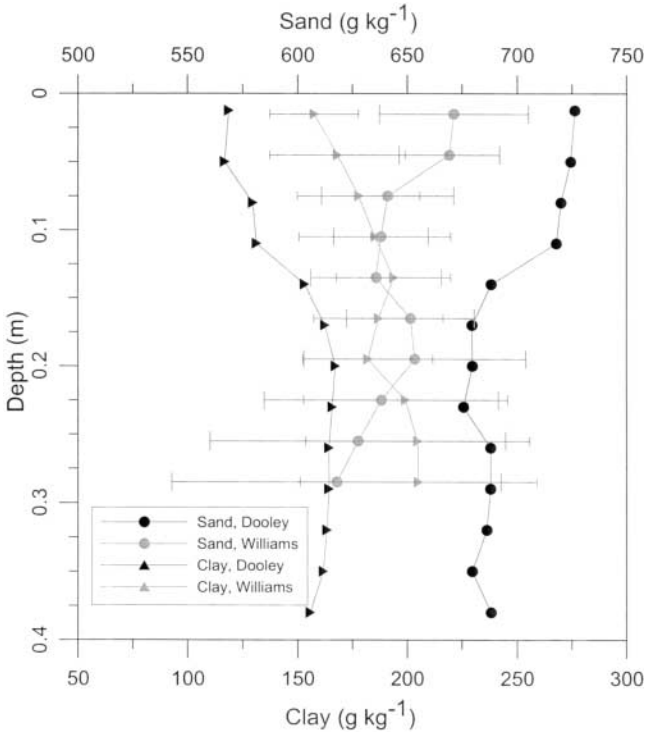

Fig. 3. Concentration of sand and clay for Dooley fine sandy loam (Exp. 1) and Williams loam (Exp. 2). Error bars indicate ± 1 SD and are shown for the Williams soil.

Soil ρ_b at 0.14 m ≈7 d after three wetting and drainage cycles was 1.44 Mg m^{-3} for SSplus, 1.15 Mg m^{-3} for SS, and 1.64 Mg m^{-3} for NoSS treatments. Results suggest that soil, within the subsoiled zone under SSplus, consolidated following three artificial rainstorms. Our water infiltration measurements support these observations.

Vertical sampling (Exp. 2) in the rip zone was not possible because of the difficulty in obtaining a representative soil core. Samples for this experiment were taken ≈0.20 m off-center of the subsoiled rip. There were no differences in soil ρ_b among treatments (Fig. 2). In comparison of SSplus and SS to NoSS, these measurements suggest that the soil was not loosened 0.20 m either side of the parabolic subsoiling shank (Fig. 2).

Differences in soil water content can cause differences in soil strength. Our soil water measurements (θ_v) and ρ_b measurements were taken concurrently with PR measurements. Profiles of θ_v (Fig. 1 and 2) show little difference among treatments. Differences in PR are therefore expected to be a consequence of soil subsidence or soil loosening.

Penetration Resistance

Penetration resistance measurements were used as an index of soil subsidence following three consecutive artificial rainstorms. Measurements were mapped as a three-dimensional surface plot to visualize tillage induced soil structure and as a way to quantify changes in structure as a consequence of repeated wetting and drainage. Examples of these maps for Exp. 1 are shown in Fig. 4 for soil under NoSS and Fig. 5 for soil under SS.

The tillage pan approximately between the 0.075- and 0.175-m depth is evident in Fig. 4. Increases in PR at this depth across a 0.42-m transect shows that the tillage

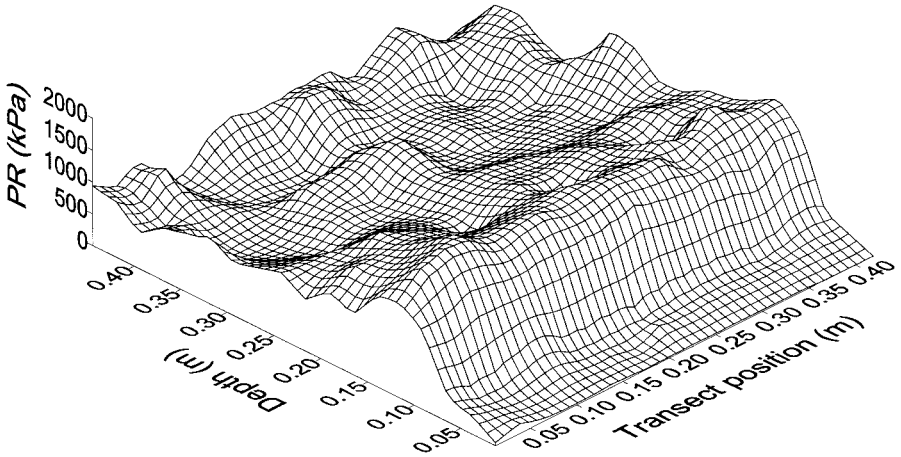

Fig. 4. Example of a smoothed surface map (Exp. 1, Dooley fine sandy loam) of penetration resistance (PR) on plots that were not subsoiled (NoSS). The bulge in PR at a depth of ≈0.15 m corresponds to the depth of a tillage pan.

pan was uniformly present within the infiltration test plot. This same pronounced pan feature was present on other test plots for both experiments (data not shown). The bulge in soil ρ_b shown for NoSS in Fig. 1 and Fig. 2 corresponds to the depth of maximum PR. Together, measurements of PR and ρ_b suggest that the tillage pan is a layer of low total porosity rather than a layer of high strength due to cementation of the soil fabric.

Tillage-induced structure provides preferential water flow paths which are important to maintain rapid water infiltration. As will be shown, either paratill subsoiling (Exp. 1) or ripping with a parabolic subsoiling shank (Exp. 2) created flow paths by fracturing the tillage pan. An example of a surface map of transect position (x), soil depth (y), and PR (z) for SS in Exp. 1 is shown in Fig. 5. Measurements followed three artificial rainstorms. This figure shows the cross-sectional area disturbed by the paratill. In this figure, the chisel portion of the subsoil shank is centered at about transect position 0.22 m. Low PR values outline a zone of soil that was fractured by the subsoil tool. This zone is roughly in the shape of a vee, extending upward and outward to the surface from a depth of ≈0.30 m (Fig. 5).

A single-value index of soil subsidence (SSI, Eq. [1]) was calculated using surface maps of the type shown in Fig. 4 and 5. For the illustrated case on Exp. 1, SSR for NoSS (Fig. 4) was 151 253 and 90 460 N for SS (Fig. 5), resulting in an SSI of 0.40 for the SS treatment. In the case of SSplus (not shown) SSI was −0.026. Values of SSI approach zero as differences between NoSS and tillage treatment become less. The combination of secondary tillage and three wetting and drainage cycles on the SSplus treatment were enough to destroy structure created by subsoiling.

On Exp. 2, before water application, average SSI was 0.37 under SS and 0.30 under SSplus, showing that sweep tillage following subsoiling reconsolidated soil disturbed by tillage, and likely destroyed some surface-connected macropores. Following three artificial rainstorms, average SSI decreased to 0.206 on SS and 0.188 on SSplus (significant at $P = 0.088$). These results indirectly suggest that there were differences in tillage-induced soil

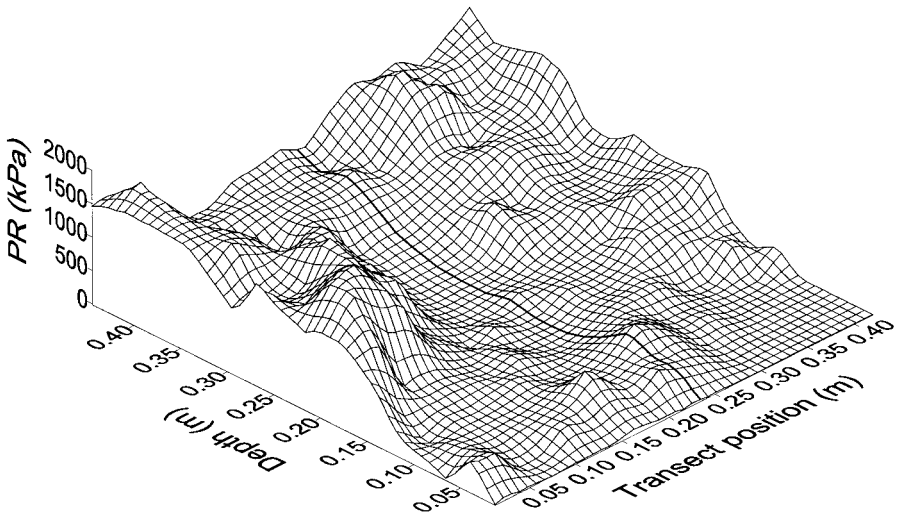

Fig. 5. Example of a smoothed surface map (Exp. 1, Dooley fine sandy loam) of penetration resistance (PR) on plots that were subsoiled (SS). The chisel portion of the paratill shank was centered at about transect position 0.22 m (shown as a bold grid-line extending from the surface to the 0.44-m depth).

Table 1. Final infiltration rate and cumulative infiltration during simulated rainstorms on three consecutive days for Exp. 1 and 2. Soil water change measured in the top 1.83 m from start to finish of 3-h infiltration tests in Exp. 2.

Consecutive day of infiltration test and treatment	Final infiltration rate†	Cumulative infiltration‡	Soil water change
	mm h^{-1}	mm	
Experiment 1, Dooley fine sandy loam			
Day 1			
Subsoiled plus	34.6	117.6	
Subsoiled	41.7	126.1	
Not subsoiled§	29.6, 32.1	83.9, 93.3	
P-value	ns	ns	
Day 2			
Subsoiled plus	7.4	47.9	
Subsoiled	40.1	122.7	
Not subsoiled§	16.0, 19.2	57.1, 62.9	
P-value	0.001	0.001	
Day 3			
Subsoiled plus	6.2	29.5	
Subsoiled	30.2	96.4	
Not subsoiled§	–	–	
P-value	0.012	0.009	
Experiment 2, Williams loam			
Day 1			
Subsoiled plus	37.8	130.2	100.8
Subsoiled	40.9	127.3	117.4
Not subsoiled	27.2	104.8	79.9
P-value	0.082	ns	0.018
Day 2			
Subsoiled plus	6.8	40.6	21.2
Subsoiled	17.0	69.8	38.6
Not subsoiled	7.2	38.1	22.3
P-value	0.001	0.002	0.001
Day 3			
Subsoiled plus	3.8	26.4	19.0
Subsoiled	11.4	50.8	26.2
Not subsoiled	5.9	31.7	18.2
P-value	0.053	0.041	0.011

† Final infiltration rate calculated as an average infiltration rate during the last hour of a 3-h infiltration test.
‡ Cumulative water infiltration during a 3-hr infiltration test.
§ On Exp. 1, only duplicate (duplicate values shown separated by comma) infiltration measurements were made on plots not subsoiled on Days 1 and 2.

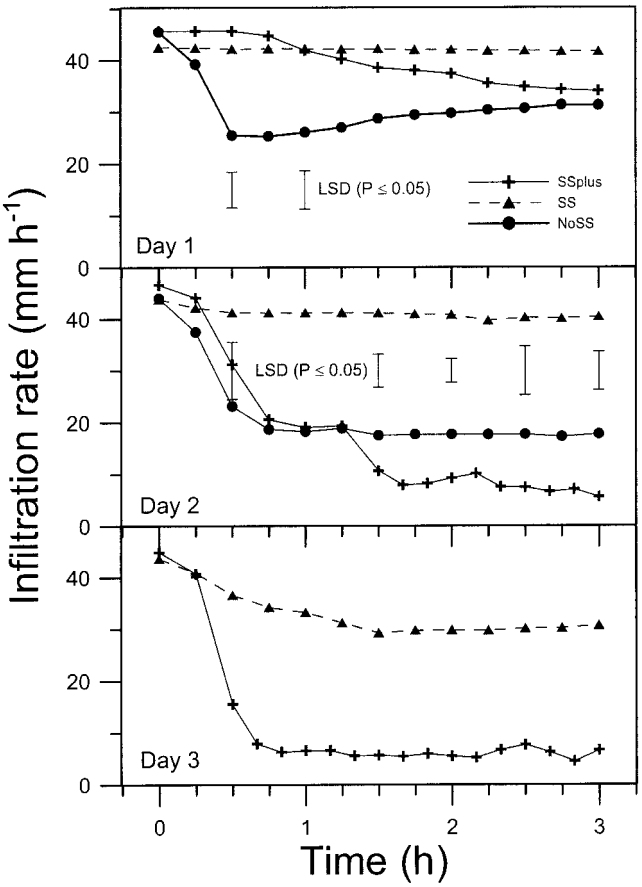

Fig. 6. Water infiltration rate during 3-h simulated rainstorms on three consecutive days on the Dooley fine sandy loam (Exp. 1). Tillage treatments were: (i) subsoiling with a paratill and secondary tillage with a disk (SSplus), (ii) subsoiling with a paratill (SS), and (iii) not subsoiled (NoSS). Least significant differences are shown for Days 1 and 2 at 0.5-h intervals where $P \leq 0.05$. Infiltration rates were significantly different between SS and SSplus for all times ≥0.5 h (ANOVA, $P \leq 0.05$) during Day 3.

structure between the two tillage treatments following the simulated rainstorms. Surface tillage (sweeps) on SSplus produced a relatively smooth surface that slaked quickly, as evidenced by reduced SSI and, as will be shown, water infiltration.

Water Infiltration and Storage

Measured water infiltration rates support local observations. Early in the growing season, runoff is rarely seen; by midsummer, however, runoff can be severe on smooth tilled fields after high-intensity thunderstorms. Infiltration measurements (Table 1) show that final infiltration on all treatments decreased with each subsequent artificial rain. On the SSplus, Exp. 1, final infiltration rate decreased from 34.6 mm h^{-1} on Day 1 to 6.2 mm h^{-1} on Day 3. Similarly, in Exp. 2, final infiltration decreased from 37.8 mm h^{-1} on Day 1 to 3.8 mm h^{-1} on Day 3. Final infiltration rate on SS for Day 3 was nearly five times greater than SSplus in Exp. 1 and three times greater than SSplus in Exp. 2.

Water infiltration was consistently greater under SS compared with SSplus and NoSS. Infiltration rates during each 3-h infiltration test for each treatment are shown in Fig. 6 and Fig. 7 for Exp. 1 and 2, respectively. These measurements, together with ρ_b and PR, provide evidence that tillage-induced preferential flow paths, continuous with the soil surface, likely contributed to the greater water infiltration under SS treatment. For tests conducted in both Exp. 1 and 2, there was a marked decrease in water infiltration on Day 2. Tests on Day 1 are difficult to interpret because differences in profile water content among treatments affect water infiltration. Following water application on Day 1 (Exp. 2), water content in the top 1.83 m was 516 mm on SSplus, 521 mm on SS, and 501 mm on NoSS (Fig. 8). The decline in infiltration on Day 2 (Exp. 2) likely reflects a change in pore space configuration at the surface because soil water content was nearly the same among treatments.

In a previous study conducted on the Dooley soil (soil of Exp. 1), we suggested that this sandy soil settled very firmly following rainfall, possibly due to the low organic matter levels and gradation of sand, silt and clay (Pikul and Aase, 1995). In the top 0.03-m layer, the Dooley soil averaged 1.5% very coarse sand, 3% coarse sand, 13% medium sand, 33% fine sand, 14% very fine sand,

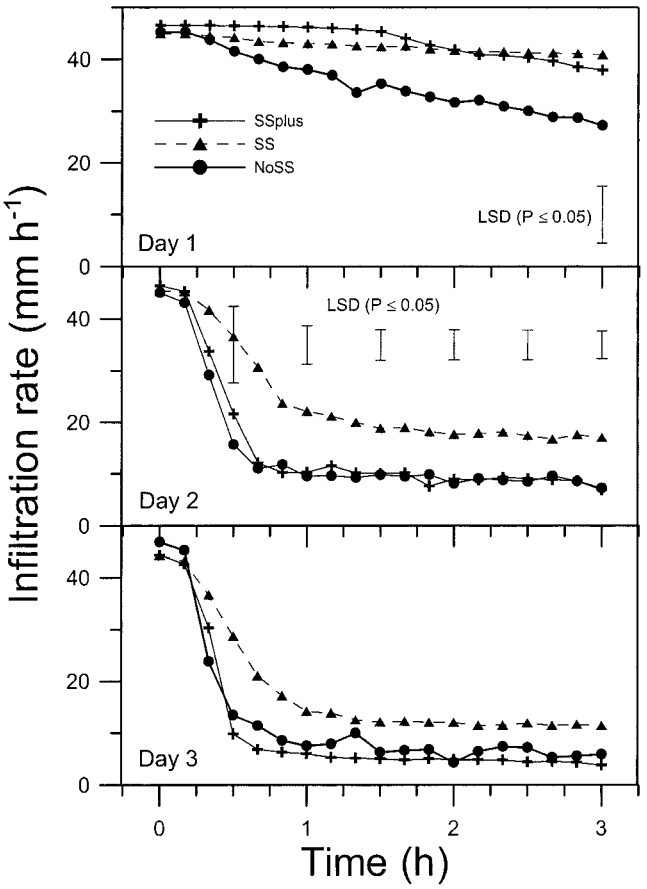

Fig. 7. Water infiltration rate during 3-h simulated rainstorms on three consecutive days on the Williams loam (Exp. 2). Tillage treatments were: (i) subsoiling with parabolic subsoiling shanks and secondary tillage with sweeps (SSplus), (ii) subsoiling with parabolic subsoiling shanks (SS), and (iii) not subsoiled (NoSS). Least significant differences are shown at 0.5-h intervals where $P \leq 0.05$.

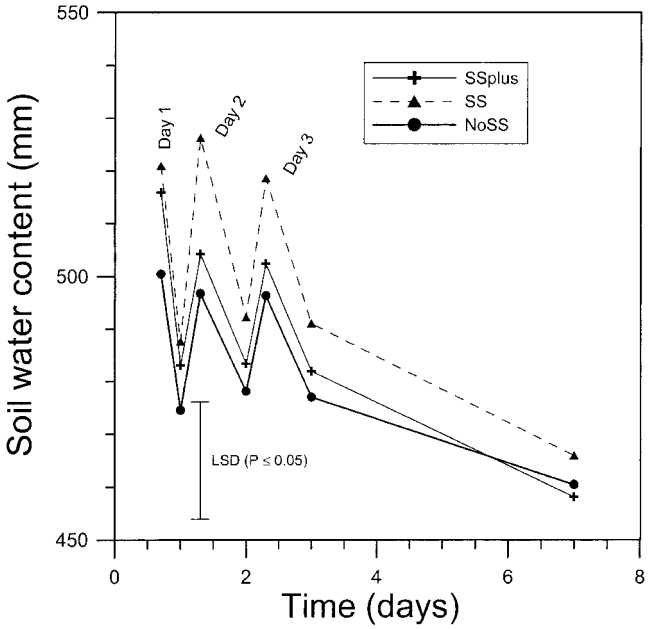

Fig. 8. Soil water content of the top 1.83 m during and after simulated rainstorms on the Williams loam (Exp. 2). Soil water measurements taken immediately after a 3-h simulated rainstorm are labeled Day 1, Day 2, and Day 3. Tillage treatments were: (i) subsoiling with parabolic subsoiling shanks and secondary tillage with sweeps (SSplus), (ii) subsoiling with parabolic subsoiling shanks (SS), and (iii) not subsoiled (NoSS). Least significant differences are shown where $P \leq 0.05$.

20% silt, and 12% clay. This textural makeup has the size components to effectively fill the available void space with solids. We believe the decline in water infiltration in the current study to be a consequence of both surface sealing and rearrangement of soil particles, or filtration of finer particles into soil pores, as water moved into the profile. These sealing processes have been described by Gupta et al. (1992).

Measured change in soil water content (Exp. 2) following each infiltration test was generally less than measured cumulative water infiltration (Table 1). For example, on Day 2, cumulative water infiltration (water addition) under SS was 69.8 mm, and measured change in soil water of the top 1.83 m was only 38.6 mm. Results were similar for other tillage treatments and suggest that internal soil water drainage was very rapid. Regardless of large differences among treatments in cumulative water infiltration (Table 1), soil profile water content (top 1.83 m) returned to ≈480 mm within a day following water application on all treatments (Fig. 8). Average drainage rate was 1.4 mm h^{-1} following infiltration tests on Days 2 and 3. During the following 4 d, water drained from the profile at a rate of 0.23 mm h^{-1}. Subsequent drainage (Days 7 to 15) was at a rate of 0.09 mm h^{-1} (Data not shown in Fig. 8) with a final measured water content of 444 mm on Day 15 (data not shown in Fig. 8).

Water infiltration (Table 1) and drainage characteristics (Fig. 8) provide evidence that runoff and deep percolation occur rapidly on the Williams loam. These data have important bearing on the conduct of water balance studies (crop water use). Neutron access tubes are often used to measure soil water status at the beginning and ending of a cropping period. Soil water status and precipitation provide the information required to calculate crop water use or soil water storage. Often, out of necessity and for lack of better information, researchers (including the authors of this report) claim that water runoff and deep percolation were negligible (Aase and Pikul, 2000; Pikul et al., 2000). Knowing the upper drained limit of a soil as suggested by Aase and Pikul (2000) and as shown here can help identify those rain events where runoff and drainage might not be negligible.

On a large-scale crop rotation experiment involving 76 plots on this same research farm (Williams loam), soil-water use was measured under six crop rotations across 5 yr (Aase and Pikul, 2000). We found that spring soil-water content (top 1.8 m) at the end of 5 yr in each rotation sequence was nearly the same as that measured in Year 1. Experimental evidence led us to the conclusion that this soil can hold only ≈450 mm of water in the top 1.83 m (0.25 m m^{-3}). Results from the current small-plot infiltration experiment support this finding.

Soil developed from glacial till has large variations in soil texture (Aase and Pikul, 2000) that causes variability in soil water storage and hydraulic conductivity. Wa-

ter draining past the root zone has implications for development of saline seeps and leaching of excess nutrients (Brown et al., 1983). On annual wheat vs. wheat–fallow rotation on this farm we found that plots under wheat–fallow had 257 kg ha^{-1} more NO_3–N in soil between the depths of 1.2 and 3.4 m than plots under annual wheat with spring tillage (Pikul and Aase, 1994, unpublished data). Primarily, spring wheat extracts the bulk of its nutrients and water from the top 1.2 m, so nutrients at depths greater than 1.2 m may be unavailable for spring wheat. Our results show that soil water in excess of ≈444 mm in the top 1.83-m profile drained quickly and this drainage could account for NO_3–N leaching from the upper profile and accumulation of nutrients in lower portions of the profile.

CONCLUSION

Efficient water management on this soil and other soils requires careful attention to: (i) soil water use by crops, (ii) reduction of erosive water runoff events, and (iii) opportunities to improve soil water recharge. In previous studies, we investigated water use characteristics of alternate crop rotations (Aase and Pikul; 1995, 2000) and use of special tillage to improve crop response or minimize spring water runoff (Pikul and Aase; 1998, 1999). In this study we have shown that water infiltration was improved by subsoiling, but subsequent tillage destroyed vertical continuity of macropore channels and reduced water infiltration on SSplus compared with SS. Our hypothesis was that tillage-induced soil macropores provide important preferential flow paths through slowly permeable soil layers and thereby increase water infiltration. Both of these soils have little structure and are susceptible to surface crusting, even with artificial rainfall that was less intense than naturally occurring storms. Smooth surface conditions following disk tillage (Exp. 1) or sweep tillage (Exp. 2) were a detriment to water infiltration because the surface rapidly slaked during the first of three artificial rainstorms. Results reveal a difficult soil management problem. Subsoil tillage improves water infiltration, but benefits of subsoiling on water infiltration were reduced by secondary tillage. Further, no additional water storage was discernable in any treatment after a short time and excess water percolation may cause leaching of nutrients. We have shown that there is an upper limit to the quantity of water that can be stored in this soil and have suggested that nutrient leaching is an inherent problem in this area. Deep-rooted crops like alfalfa, sunflower, and safflower could be used to extract water and nutrients at soil depths beyond the rooting depth of wheat. Additionally, annual cropping might be the most practical way to efficiently utilize precipitation in this semiarid agricultural region.

ACKNOWLEDGMENTS

We thank David Harris, Agricultural Research Technician, for careful maintenance of the tillage experiment and Dennis Lokken, Biological Research Technician, for assistance with infiltration experiments.

REFERENCES

Aase, J.K., and J.L. Pikul, Jr. 1995. Crop and soil response to long-term tillage practices in the Northern Great Plains. Agron. J. 87:652–656.

Aase, J.K., and J.L. Pikul, Jr. 2000. Water use in a modified summer fallow system on semiarid Northern Great Plains. Agric. Water Manage. 43:345–357.

Aase, J.K., and G.M. Schaefer. 1996. Economics of tillage practices and spring wheat and barley crop sequence in the northern Great Plains. J. Soil Water Conserv. 51:167–170.

Allmaras, R.R., J.L. Pikul, Jr., J.M. Kraft, and D.E. Wilkins. 1988. A method for measuring incorporated crop residue and associated soil properties. Soil Sci. Soc. Am. J. 52:1128–1133.

Bradford, J.M. 1980. The penetration resistance in a soil with well-defined structural units. Soil Sci. Soc. Am. J. 44:601–606.

Brown, P.L., A.D. Halvorson, F.H. Siddoway, H.F. Mayland, and M.R. Miller. 1983. Saline seeps diagnosis, control, and reclamation. USDA Conserv. Res. Rep. 30. U.S. Gov. Print. Office, Washington, DC.

Bubenzer, G.D., M. Molnau, and D.K. McCool. 1985. Low intensity rainfall with a rotating disk simulator. Trans. ASAE 28:35–43.

Busscher, W.J., R.E. Sojka, and C.W. Doty. 1986. Residual effects of tillage on coastal plain soil strength. Soil Sci. 141:144–148.

Gardner, W.H. 1986. Water Content. p. 493–544. *In* A. Klute (ed.) Methods of soil analysis. Part I. 2nd ed. Agron. Monogr. 9. ASA and SSSA, Madison, WI.

Gupta, S.C., J.F. Moncrief, and R.P. Ewing. 1992. Soil crusting in the midwestern United States. p. 205–231. *In* M.E. Sumner and B.A. Stewart (ed.) Soil crusting: Chemical and physical processes. Lewis Publ., Boca Raton, FL.

Haas, H.J., W.O. Willis, and J.J. Bond. 1974. Summer fallow in the Northern Great Plains (spring wheat). p. 12–35. *In* Summer fallow in the Western United States. USDA Conserv. Res. Rep. No. 27. U.S. Gov. Print. Office, Washington, DC.

Onstad, C.A., M.L. Wolfe, C.L. Larson, and D.C. Slack. 1984. Tilled soil subsidence during repeated wetting. Trans. ASAE 27:733–736.

Pikul, J.L., Jr., and J.K. Aase. 1995. Infiltration and soil properties as affected by annual cropping in the Northern Great Plains. Agron. J. 87:656–662.

Pikul, J.L., Jr., and J.K. Aase. 1998. Fall contour ripping increases water infiltration into frozen soil. Soil Sci. Soc. Am. J. 62:1017–1024.

Pikul, J.L., and J.K. Aase. 1999. Wheat response and residual soil properties following subsoiling of a sandy loam in eastern Montana. Soil Tillage Res. 51:61–70.

Pikul, J.L., Jr., L. Carpenter-Boggs, M. Vigil, T.E. Schumacher, M.J. Lindstrom, and W.E. Riedell. 2000. Crop yield and soil condition under ridge and chisel-plow tillage in the Northern Corn Belt, USA. Soil Tillage Res. 60(1–2):21–33.

Pikul, J.L., Jr., J.F. Zuzel, and R.E. Ramig. 1990. Effect of tillage induced soil macroporosity on water infiltration. Soil Tillage Res. 17:153–165.

Rasmussen, P.E., and W.J. Parton. 1994. Long-term tillage effects of residue management in wheat–fallow: I. Inputs, yield, and soil organic matter. Soil Sci. Soc. Am. J. 58:523–530.

Sojka, R.E., W.J. Busscher, D.T. Gooden, and W.H. Morrison. 1990. Subsoiling for sunflower production in the Southeast Coastal Plains. Soil Sci. Soc. Am. J. 54:1107–1112.

Sojka, R.E., D.T. Westerman, M.J. Brown, and B.D. Meek. 1993. Zone subsoiling effects on infiltration, runoff, erosion, and yields of furrow-irrigated potatoes. Soil Tillage Res. 25:351–368.

Tanaka, D.L. 1985. Chemical and stubble-mulch fallow influences on seasonal soil water contents. Soil Sci. Soc. Am. J. 49:728–733.

Tanaka, D.L., and J.K. Aase. 1987. Fallow method influences on soil water and precipitation storage efficiency. Soil Tillage Res. 9:307–316.

Unger, P.W. 1993a. Reconsolidation of a Torrertic Paleustoll after tillage with a Paratill. Soil Sci. Soc. Am. J. 57:195–199.

Unger, P.W. 1993b. Paratill effects on loosening of a Torrertic Paleustoll. Soil Tillage Res. 26:1–9.

Wischmeier, W.H., and D.D. Smith. 1958. Rainfall energy and its relationship to soil loss. Trans. Am. Geophys. Union 39:285–291.